Journal of Molecular Catalysis A: Chemical 359 (2012) 81–87

Contents lists available at SciVerse ScienceDirect

Journal of Molecular Catalysis A: Chemical

journal homepage: www.elsevier.com/locate/molcata

One-pot solvothermal synthesis of Pd/Fe_3O_4 nanocomposite and its magnetically recyclable and efficient catalysis for Suzuki reactions

Shaozhong Li[a], Wei Zhang[a], Man-Ho So[b], Chi-Ming Che[b], Runming Wang[a], Rong Chen[a,*]

[a] *Key Laboratory for Green Chemical Process of Ministry of Education and School of Chemical Engineering & Pharmacy, Wuhan Institute of Technology, Wuhan 430073, PR China*
[b] *Department of Chemistry and State Key Laboratory of Synthetic Chemistry, The University of Hong Kong, Pokfulam Road, Hong Kong Special Administrative Region*

ARTICLE INFO

Article history:
Received 20 January 2012
Received in revised form 6 March 2012
Accepted 25 March 2012
Available online 4 April 2012

Keywords:
Pd/Fe_3O_4
Nanocomposite
Catalysis
Recyclable
Suzuki reaction

ABSTRACT

A facile solvothermal synthetic route has been successfully developed to fabricate Pd/Fe_3O_4 nanocomposite with the assistance of polyvinylpyrrolidone (PVP) in N,N-dimethylformamide (DMF) solution. The as-prepared Pd/Fe_3O_4 nanocomposite was composed of uniform 5 nm-sized Pd nanoparticles and Fe_3O_4 nanocrystals with dimension of 40 nm. In this fabrication, PVP played an important role as a capping agent. The as-prepared Pd/Fe_3O_4 nanocomposite exhibited superior catalytic performance and stability for various Suzuki coupling reactions, compared with single-component Pd nanoparticles under the same reaction conditions. More importantly, it displayed good magnetic property and could be easily separated from the reaction mixture by using a magnet and recycled for 10 times without losing its catalytic activity.

1. Introduction

Recently, nanostructured catalysts have been extensively investigated due to their much higher activities than that of the corresponding bulk materials [1–5]. Compared with frequently used palladium (II) complexes catalysts, palladium nanoparticles were found to exhibit remarkable catalytic activities for Suzuki, Heck and Sonogashira cross-coupling reactions [6–11], which have been extensively used in the synthesis of drugs and fine chemicals [12–17]. However, nanosized catalysts are usually hardly separated and recovered from the reaction systems efficiently by traditional filtration and centrifugation methods. For example, the tiny palladium nanoparticles usually suffered from the problems in catalyst separation and agglomeration, which resulted in the decrease of catalytic activity and recyclable usage [18,19]. In order to overcome these drawbacks, many efforts have been devoted to synthesize nanoscaled magnetically recyclable catalysts (MRCs) in recent years, which were composed of two or more different materials. The hybrid nanocrystals realized the integration of highly catalytic activity and easy separation in MRCs. For instance, Chen and co-workers synthesized Ag–Fe_3O_4 nanocomposite as a magnetically recyclable and efficient catalyst for expoxidation of styrene [20]. Au–Fe_3O_4 heterodimer nanocrystals were also used for dual imaging probes for MRI and optical imaging [21]. Many works also demonstrated that Pd supported hybrid materials displayed higher catalytic activity and stability [22–25]. Among numerous supporting materials studied, Fe_3O_4 is of scientific and technological importance due to its intrinsic magnetic property and preeminent applications in catalysis, biotechnology and environmental remediation [26]. Up to now, different Pd/Fe_3O_4 hybrid nanocrystals were synthesized and exhibited good catalytic performance on methanol oxidation, cross-coupling reaction, cis- and trans-2-butene conversion [27–30]. Unfortunately, most reported MRCs synthetic processes involved multi-step, complicated procedures and harsh reaction conditions. Therefore, the development of facile and rapid methods for the synthesis of efficient MRCs still remains a great challenge.

Enlightened by the previous work, we reported a new simple one-pot synthesis of Pd/Fe_3O_4 nanocomposite with the assistance of polyvinylpyrrolidone (PVP). In this study, a single $FeCl_2$ precursor was used to generate Fe_3O_4 nanoparticles, which was seldom reported in the synthesis of Fe_3O_4. PVP played an important role as a capping agent in the formation of Pd/Fe_3O_4 nanocomposite, which resulted in the random distribution of Pd and Fe_3O_4 nanocrystals. Furthermore, it was found that the synthesized Pd/Fe_3O_4 nanocomposites exhibited efficient catalytic activities for various Suzuki cross-coupling reactions. The Fe_3O_4 nanocrystal was used as a support of Pd nanoparticles, as well as enhancing the dispersion of catalysis active sites and improving its catalytic activity. More importantly, the synthesized Pd/Fe_3O_4 nanocomposite presented good magnetic property, and could be easily separated from the reaction mixture by using a magnet. By utilizing this property, it

---

* Corresponding author. Tel.: +86 13659815698; fax: +86 2787195671.
E-mail address: rchenhku@hotmail.com (R. Chen).

1381-1169/$ – see front matter © 2012 Elsevier B.V. All rights reserved.
http://dx.doi.org/10.1016/j.molcata.2012.03.025

could be reused for 10 cycles without losing its catalytic activity, indicative of a potential application in industry.

2. Experimental

2.1. Chemicals

Polyvinylpyrrolidone (PVP, M.W. = 55,000), ferrous chloride tetrahydrate ($FeCl_2{\cdot}4H_2O$) and palladium chloride ($PdCl_2$) were purchased from Sigma–Aldrich. Cetyltrimethylammonium bromide (CTAB) was purchased from Lancaster. N,N-dimethylformamide (DMF), ethanol (EtOH), tetrabutyl ammonium bromide (TBAB), sodium iodide (NaI) and all the organic substrates were purchased from Aladdin (Shanghai, China). Palladium (10%) on carbon catalyst (Pd/C) was purchased from Sinopharm Chemical Reagent Co., Ltd. (Shanghai, China). All the chemicals used in the experiment were analytical grade and used without further purification.

2.2. Synthesis

In the typical synthesis, 0.0133 g $PdCl_2$ (0.075 mmol), 0.16 g PVP (M.W. = 55,000) and 0.0149 g $FeCl_2{\cdot}4H_2O$ (0.075 mmol) were added into 12 mL mixed solution which contained 10 mL DMF and 2 mL deionized water. The mixture was sonicated for 2 min to form a turbid solution, and then transferred to a 30 mL Teflon-lined stainless-steel autoclave to perform the solvothermal process at 150 °C for 8 h. After cooling down to room temperature, a black product was collected by a magnet and washed with deionized water for three times and ethanol for three times. The product was finally dried in a desiccator at room temperature for further characterization (**S1**). Other samples (**S2–S8**) were prepared under identical reaction conditions by varying surfactants and solvents.

2.3. Characterization

Powder X-ray diffraction (XRD) was carried out on a Bruker AXS D8 Discover (Cu Kα = 1.5406 Å). The scanning rate was $1^\circ\,min^{-1}$ in the 2θ range from 20 to 80°. The transmission electron microscopy (TEM), high-resolution transmission electron microscopy (HRTEM) images and selected area electron diffraction (SAED) patterns were recorded on a Philips Tecnai G2 20 electron microscope, using an accelerating voltage of 200 kV. TEM samples were prepared by dispersing some solid product into ethanol and then sonicating for approximately 30 s. A few drops of the suspension were deposited on copper grids, which were then put into the desiccators for drying. The energy-dispersive X-ray (EDX) analysis was performed on an Oxford Instruments INCA with a scanning range from 0 to 20 keV. Raman spectrum was measured by a confocal laser micro-Raman spectrometer (DXR, USA) equipped with a He–Ne laser with excitation of 532 nm. Spectrum was obtained at a laser power of 0.6 mW and a 60 s acquisition time in the wavenumber range of 50–2000 cm^{-1}. The concentration of Pd in the Pd/Fe_3O_4 nanocomposites was analyzed by inductively coupled plasma mass spectrometry (ICP-MS, Agilent ICP-MS 7500ce). The magnetic measurements were recorded on a SQUID magnetometer at 298 K, Quantum Design MPMS (see Table 1).

2.4. Suzuki coupling reactions

Catalytic activity of the synthesized Pd/Fe_3O_4 nanocomposite was tested through the Suzuki reaction of aryl halides with phenylboronic acid. In the typical experiment, a mixture of aryl halide (1.0 mmol), phenylboronic acid (1.5 mmol), tetrabutylammonium bromide (1 mmol), K_2CO_3 (2 mmol), and 5.6 mg Pd/Fe_3O_4 nanocomposite (containing 0.2%, mmol Pd) were added into 9 mL ethanol/H_2O (v/v = 1:2) solution. The reaction mixture was then refluxed under the temperature of 86 °C for 30–180 min (see Tables 2 and 3). After reaction, the reactor was cooled down to the room temperature, and the product was extracted with diethyl ether for three times. Then the organic phase was dried with anhydrous Na_2SO_4 and evaporated in vacuum. Finally, the product was obtained and purified by column chromatography using diethyl ether/petroleum ether (for yields see Tables 2 and 3). All the products were known in literatures and identified by comparing their ^1H NMR spectra with standard data. For recycle experiment, the separated Pd/Fe_3O_4 composite nanocatalyst was washed with deionized water (4 mL × 3) and ethanol (4 mL × 3), and dried in vacuum for 24 h before the re-usage.

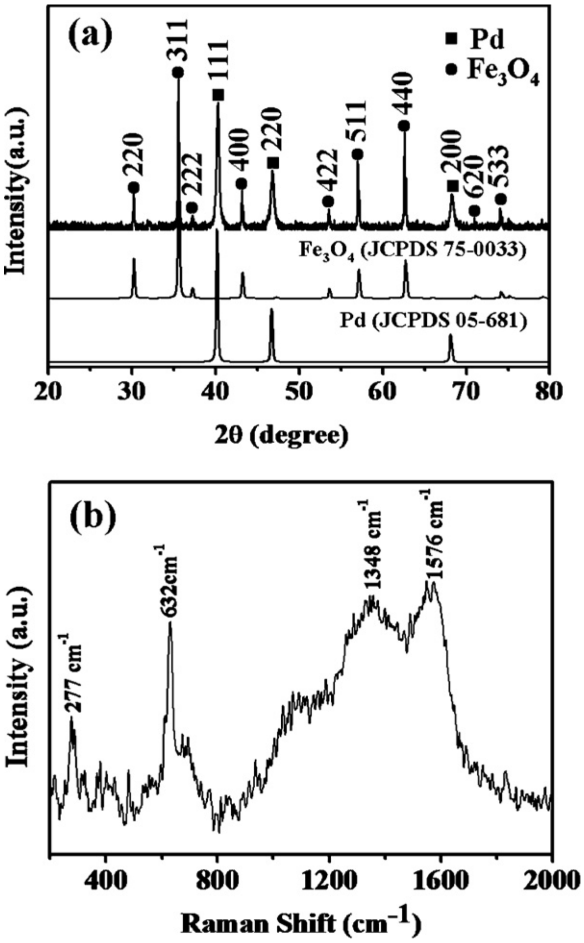

Fig. 1. XRD pattern (a) and Raman spectrum (b) of Pd/Fe_3O_4 nanocomposite synthesized by solvothermal method (**S1**).

3. Result and discussion

3.1. Structure and morphology

The composition and crystallinity of the as-synthesized product (**S1**) was characterized by the powder XRD analysis. Fig. 1a shows the typical XRD pattern of the as-synthesized product prepared by one-pot solvothermal method (**S1**). As shown in Fig. 1a, all the diffraction peaks could be readily indexed to (1 1 1), (2 0 0), (2 2 0) lattice planes of a face-centered cubic (fcc) Pd crystal structure (JCPDS 05-0681) and (2 2 0), (3 1 1), (2 2 2), (4 0 0), (5 1 1), (4 4 0) lattice planes of fcc Fe_3O_4 (JCPDS 75-0033). No other diffraction peaks was detected, indicative of the high-purity of the Pd/Fe_3O_4 nanocomposites. As both magnetite (Fe_3O_4) and maghemite

Table 1
Experimental parameters for the preparation of Pd/Fe_3O_4 nanocomposites.

Sample	Fe source	Pd source	Capping agent	Salt	Solvent
S1	$FeCl_2$	$PdCl_2$	PVP	–	DMF + H_2O
S2	–	$PdCl_2$	PVP	–	DMF + H_2O
S3	$FeCl_2$	–	PVP	–	DMF + H_2O
S4	$FeCl_2$	$PdCl_2$	PVP	–	DMF
S5	$FeCl_2$	$PdCl_2$	PVP	–	H_2O
S6	$FeCl_2$	$PdCl_2$	–	–	DMF + H_2O
S7	$FeCl_2$	$PdCl_2$	PVP	NaI	DMF + H_2O
S8	$FeCl_2$	$PdCl_2$	–	NaI	DMF + H_2O

Note: The amount of NaI was 0.3 g.

Table 2
Products and yields for Suzuki coupling reactions of phenylboronic acid and various aryl halides catalyzed by Pd/Fe_3O_4 nanocomposite (**S1**) and Pd nanoparticles ($\sim$5 nm)

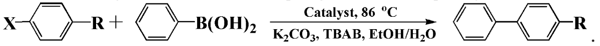

Entry	Substrates	Products	Time (h)	Isolated yield (%)	
				S1	Pd Nps
1	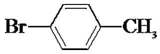	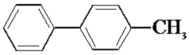	1.5	94	85
2	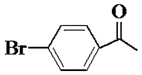	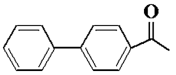	1.5	96	40
3	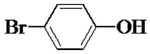	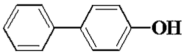	3	98	30
4	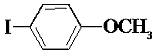	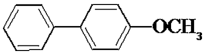	0.5	98	94
5	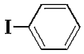	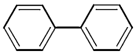	0.5	97	92

Reaction condition: a catalyst containing 0.2%, mmol Pd, aryl halide (1.0 mmol), phenylboronic acid (1.5 mmol), K_2CO_3 (2 mmol), TBAB (1 mmol), 9 mL EtOH/H_2O (v/v = 1/2) solution. T = 86 °C.

(γ-Fe_2O_3) had good magnetism and similar XRD pattern [31], Raman spectroscopy was used to distinguish the different structural phases of iron oxides. Fig. 1b illustrated the Raman spectroscopy of as-synthesized Pd/Fe_3O_4 nanocomposites (**S1**), which showed the main features at 277, 632, 1348, and 1576 cm^{-1}. The Raman peaks at 1348 and 1576 cm^{-1} were assigned to characteristic peak of palladium nanoparticles [32], and the peaks at 277 and 632 cm^{-1} were attributed to Fe_3O_4 nanocrystals, demonstrating a red-shift of 34 cm^{-1} compared with the Raman spectrum of commercial magnetite powder [33]. According to the reported literature [34], the red-shift was ascribed to a compressive strain induced by the substantial lattice mismatch between Pd and Fe_3O_4, owing to the attachment of Pd nanoparticles on Fe_3O_4 surface. It further confirmed the presence of magnetite phase.

Fig. 2 showed the typical TEM images of as-synthesized Pd/Fe_3O_4 nanocomposites (**S1**). It was observed that the Pd/Fe_3O_4 nanocomposites were composed of tiny Pd nanoparticles with an average diameter of 5 nm and faceted Fe_3O_4 nanocrystals with dimensions of about 40 nm (Fig. 2a). As shown in Fig. 2b and c, well-dispersed Pd nanoparticles were homogeneously deposited on the surface of Fe_3O_4 nanocrystals. The selected area electron diffraction (SAED) pattern of sample S1 revealed several diffraction rings, which were the sum of diffraction patterns of different Pd and Fe_3O_4 nanocrystals, thus indicative of good crystallinity (inset of Fig. 2b). The HRTEM image of the Pd/Fe_3O_4 nanocomposites (**S1**) was shown in Fig. 2d. It also clearly revealed that Pd nanoparticles were directly attached on the Fe_3O_4 nanocrystals. The lattice fringes for both Pd and Fe_3O_4 nanocrystals could be determined to be (2 0 0) planes of Pd component with a d-spacing of 0.193 nm and (1 1 1) planes of Fe_3O_4 component with a d-spacing of 0.485 nm. The elemental composition of the nanocomposite was also analyzed by the energy-dispersive X-ray (EDX) spectrum (Fig. S1, Supplementary data). It further confirmed that the Pd/Fe_3O_4 nanocomposite (**S1**) was composed of palladium, iron and oxygen. The copper and carbon signals are from the carbon-coated copper grid.

Table 3
Products and yields for Suzuki coupling reactions of phenylboronic acid and various aryl halides catalyzed by Pd/Fe_3O_4 nanocomposite (**S7**).

Entry	Substrates	Products	Time (h)	Isolated yield (%)
1	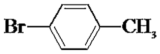	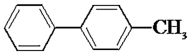	6	88
2	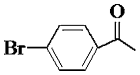	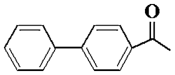	6	83
3	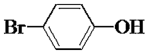	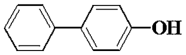	6	94
4	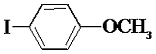	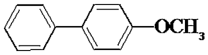	0.5	96
5	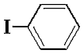	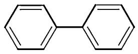	0.5	94

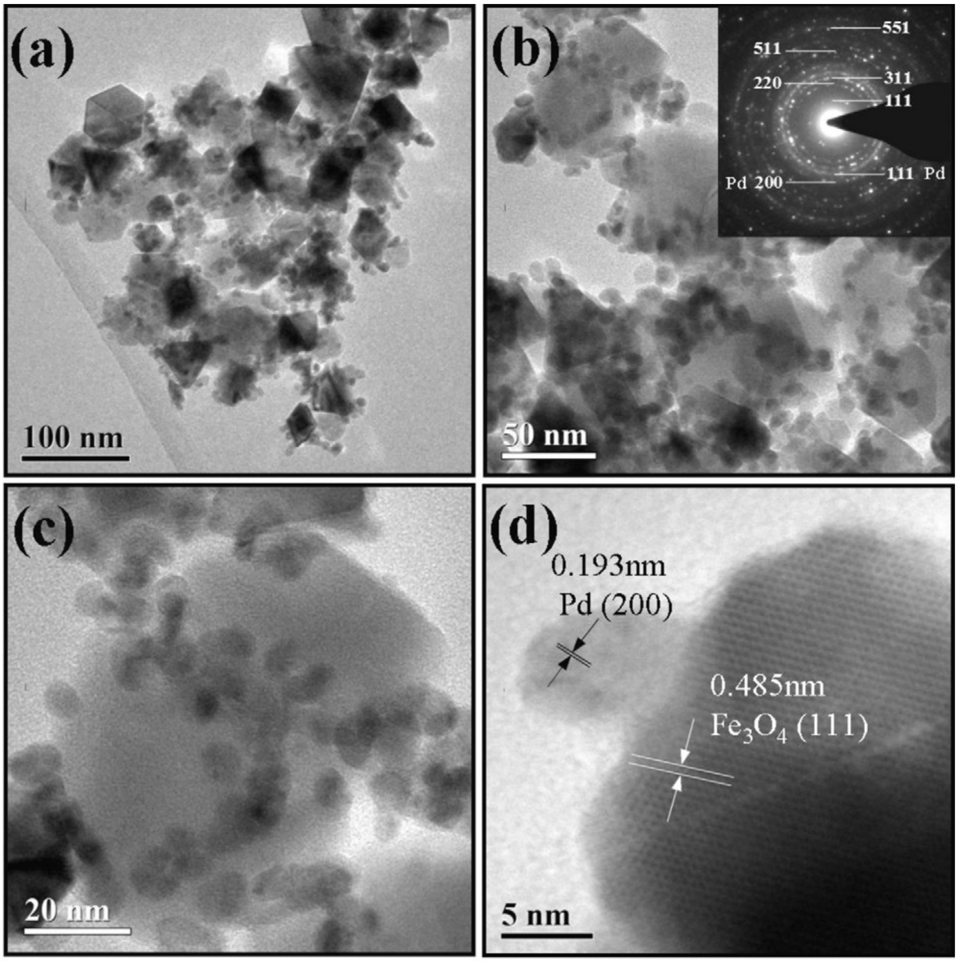

Fig. 2. TEM (a–c) and HRTEM (d) images of Pd/Fe_3O_4 nanocomposites prepared by solvothermal method (**S1**). Inset of (b) is the corresponding SAED pattern of Pd/Fe_3O_4 nanocomposite (**S1**).

In order to understand the formation mechanism and optimize the synthetic conditions, different control experiments were performed. When $PdCl_2$ was solely used as precursor, aggregated Pd nanoparticles were obtained (**S2**), in so far that DMF could act both as a solvent and a powerful reducing agent to generate Pd nanoparticles in the presence of PVP [35–39]. However, no Fe_3O_4 product was formed in the absence of palladium source under the identical condition (**S3**). It confirmed that Pd^{2+} could be reduced by $FeCl_2$ as well and Fe^{2+} ions were partly oxidized to from Fe_3O_4 nanocrystals. To further verify the speculation, a control experiment was carried out under identical conditions in pure DMF solvent and deionized water, respectively (**S4** and **S5**). No Pd/Fe_3O_4 nanocomposite was obtained in pure DMF or water solution (Fig. S2, Supplementary data). Hence, it indicated that the chemical reactions involved in the formation of Pd/Fe_3O_4 nanocomposite were as following:

$$Pd^{2+} + 2Fe^{2+} \rightarrow Pd + 2Fe^{3+}$$

$$Pd^{2+} + Me_2NCHO + H_2O \rightarrow Pd + Me_2NCOOH + 2H^+$$

$$2Fe^{3+} + Fe^{2+} + 4H_2O \rightarrow Fe_3O_4 + 8H^+$$

In this formation, PVP played an important role as a capping agent which not only contained polyvinyl skeleton, but also provided nitrogen and oxygen atoms with polar groups [40]. We also attempted to synthesize Pd/Fe_3O_4 nanocomposites in the absence of PVP. Unfortunately, it was difficult to obtain Pd/Fe_3O_4 nanocomposite coated with well-dispersed Pd nanoparticles. It was found that little Pd nanoparticles were randomly deposited on the Fe_3O_4 nanocrystals in the absence of PVP (**S6**, Fig. S3, Supplementary data). It was proposed that the polyvinyl skeleton might be readily coated on Fe_3O_4 nanocrystals through hydrophobic interactions, while the group including nitrogen and oxygen atoms absorbed on Pd plane surface due to the weak binding of PVP [41].

In this study, sodium iodide was also used in the synthesis of Pd/Fe_3O_4 nanocomposites, which could depress the spontaneous nucleation [42]. Pd/Fe_3O_4 nanocomposite was also obtained in the presence of NaI salt (**S7**), as confirmed by its XRD pattern (Fig. S4, Supplementary data). All the diffraction peaks could be readily matched with fcc phase of Fe_3O_4 (JCPDS 75-0033) and fcc phase of Pd (JCPDS 05-0681), indicative of the formation of Pd/Fe_3O_4 product. Fig. 3 shows the corresponding TEM and HRTEM images of sample S7. TEM images of Fig. 3a–c revealed that uniform Pd nanoparticles with an average diameter of 25 nm were well-dispersed on the surface of Fe_3O_4 nanocrystals. The particle size of Pd/Fe_3O_4 nanocomposites was in the range of 200–300 nm. HRTEM image of sample S7 (Fig. 3d) revealed clear lattice fringes with a *d*-spacing of 0.217 and 0.485 nm corresponding to the (1 1 1) lattice plane of fcc Pd and Fe_3O_4 respectively, indicative of good crystallinity. The corresponding SAED pattern showed different diffraction rings, which also confirmed the good crystallinity of Pd/Fe_3O_4 naocomposite (Inset of Fig. 3a). These results demonstrated that the particle sizes were larger than that of the sample S1 synthesized in the absence of NaI. It indicated that the addition

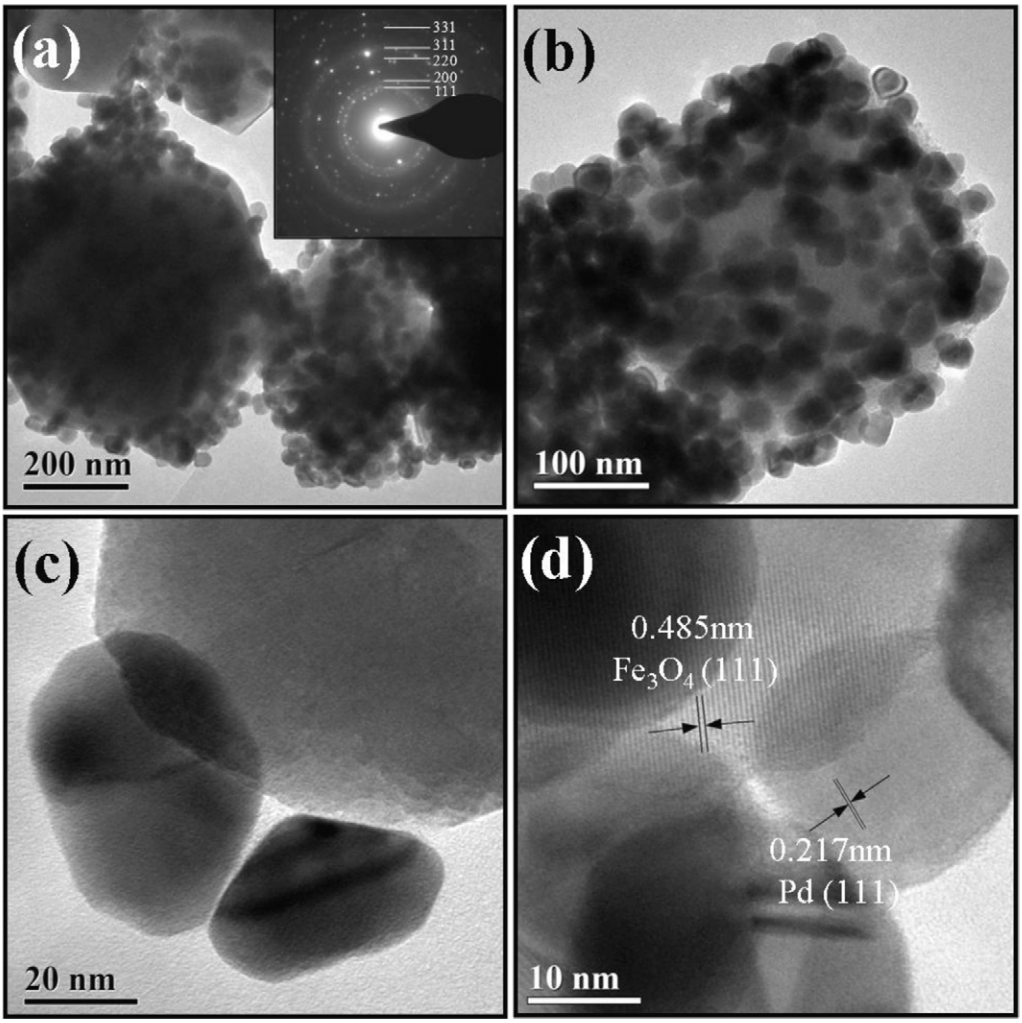

Fig. 3. TEM (a–c) and HRTEM (d) images of Pd/Fe_3O_4 nanocomposites prepared by solvothermal method in the presence of NaI (**S7**).

of NaI could depress spontaneous nucleation of Pd nanoparticles. Noticeably, Pd/Fe_3O_4 nanocomposite was hardly formed in the absence of PVP, despite the addition of NaI salt (**S8**) (Fig. S5, Supplementary data). It further verified the function of PVP as a capping agent.

3.2. ICP-MS measurement and magnetic property

The concentration of Pd in the Pd/Fe_3O_4 nanocomposite (**S1**) was determined by inductively coupled plasma mass spectrometry (ICP-MS) analysis. The ICP-MS data revealed that the relative Pd concentration in the Pd/Fe_3O_4 nanocomposite was 3.82 wt%. The magnetic property of the Pd/Fe_3O_4 nanocomposite (**S1**) was also investigated. Fig. 4 shows the hysteresis loop of Pd/Fe_3O_4 nanocomposite obtained in applied magnetic field at 298 K by using a SQUID magnetometer. The magnetic saturation value of the composite was estimated to be 53.4 emu g^{-1}. As shown in inset of Fig. 4, the Pd/Fe_3O_4 nanocomposite was easily separated from the solution, indicating that it was suitable for magnetic separation applications.

3.3. Catalytic activity

Suzuki coupling reaction is an effective and versatile synthetic route for the construction of biaryls, which involved the reaction of arylboronic acids and aryl halides. In this study, the catalytic activity of the as-prepared Pd/Fe_3O_4 nanocomposite (**S1**) was evaluated through a series of Suzuki coupling reactions in aqueous medium. Table 2 gives the reaction conditions and results for five coupling reactions. It was found that the Pd/Fe_3O_4 nanocomposite (**S1**) exhibited excellent catalytic activity for Suzuki coupling reactions of phenylboronic acid with various aryl bromides (entries 1–3 in Table 2) and aryl iodides (entries 4–5 in Table 2). The isolated yields could reach to 94–98% after 0.5–3 h refluxing at

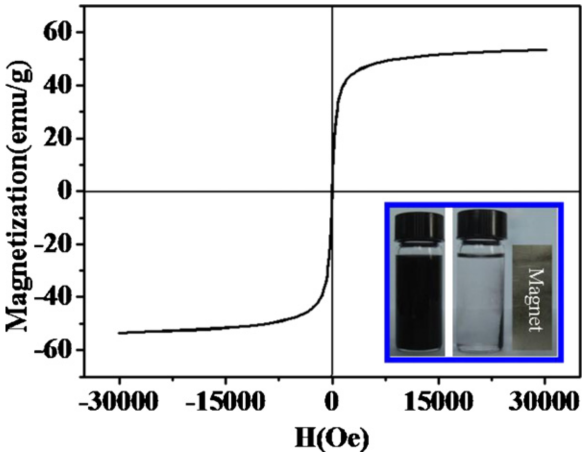

Fig. 4. Hysteresis loop of the as-prepared Pd/Fe_3O_4 nanocomposite (**S1**) at 298 K.

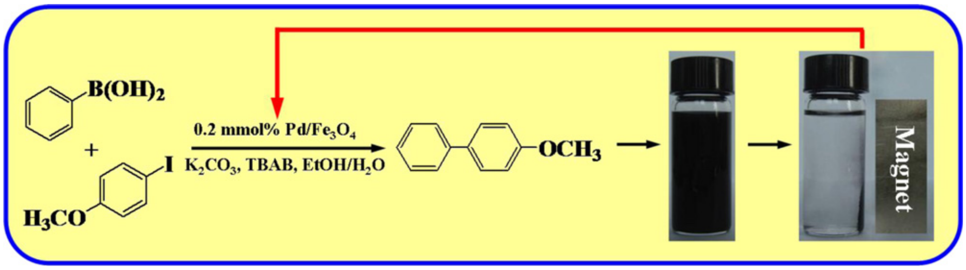

Scheme 1. Magnetic separation and recycling of Pd/Fe_3O_4 catalyzed the reaction for the cycle.

86 °C. More importantly, the Pd/Fe_3O_4 nanocomposite (**S1**) showed enhanced catalytic activity for various Suzuki reactions, compared with single-component Pd nanoparticles with the same particle size (~5 nm, Fig. S6, Supplementary data) under the identical experimental conditions. It indicated that the choice of Fe_3O_4 as catalyst support played an important role on the overall performance of the catalytic system. Fe_3O_4 nanocrystals not only provided adequate magnetic property for the separation of nanocomposites, but also enhanced the dispersion of Pd active sites, leading to the improvement of catalytic activity. In literatures, it was also reported that supported catalyst could improve its activity, selectivity or stability [23,43–45].

It was also found that the Pd/Fe_3O_4 nanocomposite (**S1**) afforded better catalytic activity than the commercial Pd/C when the same amount of Pd mol% was employed in the Suzuki reactions (Table S1, Supplementary data). Furthermore, the results implied that it was possible to maximize the catalytic activity of Pd nanoparticle through the supporting metal oxide nanocrystals, except for the control of Pd nanoparticle size and shape.

It was worth noting that the catalytic activity of Pd/Fe_3O_4 nanocomposite prepared in the presence of NaI (**S7**) was obviously lower than that of sample S1. Although it remained similar catalytic activity for aryl iodides (entries 4–5 in Table 3), the Suzuki reactions of phenylboronic acid with aryl bromides only afforded the coupling product in 88%, 83%, and 94% isolated yield, respectively, even after 6 h refluxing (entries 1–3 in Table 3). These results demonstrated that the Pd/Fe_3O_4 nanocomposite (**S7**) showed a decrease in catalytic activity, compared with sample S1. It was proposed that the increase of particle size resulted in the decrease of catalytic activity [46,47].

Due to the good magnetic performance, Pd/Fe_3O_4 nanocomposite was very useful for overcoming the intrinsic difficulty associated with the separation of homogeneous Pd (II) complex based and Pd nanoparticles based catalysts in Suzuki coupling reactions. Hence, the recycle of Pd/Fe_3O_4 nanocomposite was investigated. We have carried out recycling uses of the Pd/Fe_3O_4 nanocomposite (**S1**) catalyst for the Suzuki reaction of 4-iodophenyl methyl ether with phenylboronic acid, and the coupling product was obtained with a yield of 98% in the first cycle. When the Suzuki coupling reaction was completed, the Pd/Fe_3O_4 nanocomposite (**S1**) catalyst could be easily separated from the reaction mixture by using a magnet (Scheme 1), then washed and dried for re-usage. The recycled Pd/Fe_3O_4 catalyst was then used in model reaction under the same reaction conditions, and it could be recycled for many times without losing its catalytic activity. As depicted in Fig. 5, the catalyst (**S1**) still remained excellent catalytic activity even after 10 times of recycling. The recycling model reaction of phenylboronic acid with 4-iodophenyl methyl ether was also carried out under identical conditions by using the Pd/Fe_3O_4 nanocomposite (**S7**) and commercial Pd/C as a catalyst, respectively. Pd/Fe_3O_4 nanocomposite (**S7**) was recycled the Suzuki coupling reaction for 7 times, and afforded good yield of 86% after six recycles. The isolated yield decreased to 41% in the 7th recycling reaction. It indicated that the large particle size of Pd/Fe_3O_4 nanocomposite also easily resulted in the loss of catalytic activity in the recycling use. Meanwhile, the commercial Pd/C catalyst could only be reused for 5 times and lose its high catalytic activity in the 6th recycling reaction.

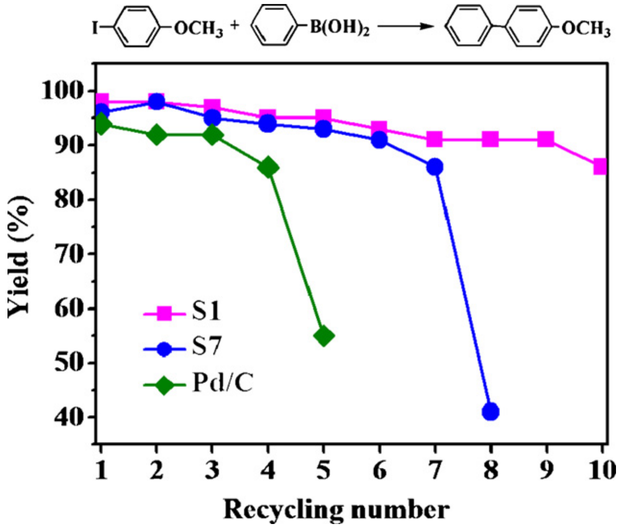

Fig. 5. Recycling results of Suzuki coupling reaction of phenylboronic acid with 4-iodophenyl methyl ether over different Pd/Fe_3O_4 nanocomposite (**S1** and **S7**) and Pd/C catalysts.

4. Conclusions

In summary, we developed a facile one-pot solvothermal route to synthesize Pd/Fe_3O_4 nanocomposite from $FeCl_2$ and $PdCl_2$ in the presence of PVP for the first time. Uniform Pd nanoparticles were well-dispersed on the surfaces of Fe_3O_4 nanocrystals to form Pd/Fe_3O_4 nanocomposite. In this fabrication, PVP played an important role as a capping agent in the formation of Pd/Fe_3O_4 nanocomposite. The as-prepared Pd/Fe_3O_4 nanocomposite exhibited excellent catalytic activity for various Suzuki coupling reactions. More importantly, the Pd/Fe_3O_4 nanocomposite displayed good magnetic property, which facilitated the collection by magnetic method. It could be easily separated by a magnet when the Suzuki coupling reactions completed, and then recycled for 10 times without losing its catalytic activity. This work provides a new synthetic strategy for the fabrication of magnetically recyclable Pd/Fe_3O_4 nanocomposites, which could be applied to many important industrial catalytic processes and extended to achieve the synthesis of various noble-metal/Fe_3O_4 nanocomposites.

Acknowledgements

This work was supported by Program for New Century Excellent Talents in University (NCET-09-0136), National Natural Science Foundation of China (21171136) and Key Program of Hubei Provincial Department of Education (D20111510).

Appendix A. Supplementary data

Supplementary data associated with this article can be found, in the online version, at doi:10.1016/j.molcata.2012.03.025.

References

[1] (a) M.K.W. Chi, W.Y. Yu, M.H. So, C.Y. Zhou, Q.M. Deng, C.M. Che, Chem. Asian. J. 3 (2008) 1256–1265;
(b) M.H. So, Y.G. Liu, C.M. Ho, C.M. Che, Chem. Asian. J. 4 (2009) 1551–1561;
(c) M.H. So, Y.G. Liu, C.M. Ho, K.Y. Lam, C.M. Che, ChemCatChem 3 (2011) 386–393;
(d) L.N. Lewis, Chem. Rev. 93 (1993) 2693–2730.
[2] T.M. Trnka, R.H. Grubbs, Acc. Chem. Res. 34 (2000) 18–29.
[3] M.D. Malinsky, K.L. Kelly, G.C. Schatz, R.P. Van Duyne, J. Am. Chem. Soc. 123 (2001) 1471–1482.
[4] W.P. McConnell, J.P. Novak, L.C. Brousseau, R.R. Fuierer, R.C. Tenent, D.L. Feldheim, J. Phys. Chem. B 104 (2000) 8925–8930.
[5] F. Shi, M.K. Tse, M.M. Pohl, J. Radnik, A. Bruckner, S. Zhang, M. Beller, J. Mol. Catal. A: Chem. 292 (2008) 28–35.
[6] W. Zhang, Q. Wang, F. Qin, H. Zhou, Z. Lu, R. Chen, J. Nanosci. Nanotechnol. 11 (2011) 7794–7801.
[7] K. Sawai, R. Tatumi, T. Nakahodo, H. Fujihara, Angew. Chem. Int. Ed. 120 (2008) 7023–7025.
[8] C. Evangelisti, N. Panziera, P. Pertici, G. Vitulli, P. Salvadori, C. Battocchio, G. Polzonetti, J. Catal. 262 (2009) 287–293.
[9] Y. Li, X.M. Hong, D.M. Collard, M.A. El-Sayed, Org. Lett. 2 (2000) 2385–2388.
[10] R. Tatumi, T. Akita, H. Fujihara, Chem. Commun. (2006) 3349–3351.
[11] V. Calò, A. Nacci, A. Monopoli, P. Cotugno, Angew. Chem. Int. Ed. 48 (2009) 6101–6103.
[12] N. Miyaura, A. Suzuki, Chem. Rev. 95 (1995) 2457–2483.
[13] A. Suzuki, J. Organomet. Chem. 576 (1999) 147–168.
[14] J.P. Tremblay-Morin, H. Ali, J.E. van Lier, Tetrahedron Lett. 47 (2006) 3043–3046.
[15] S. Lightowler, M. Hird, Chem. Mater. 17 (2005) 5538–5549.
[16] X. Zhan, S. Wang, Y. Liu, X. Wu, D. Zhu, Chem. Mater. 15 (2003) 1963–1969.
[17] S.D. Walker, T.E. Barder, J.R. Martinelli, S.L. Buchwald, Angew. Chem. Int. Ed. 43 (2004) 1871–1876.
[18] H. Zhang, Q. Zhu, Y. Zhang, Y. Wang, L. Zhao, B. Yu, Adv. Funct. Mater. 17 (2007) 2766–2771.
[19] Y. Feng, L. Li, Y. Li, W. Zhao, J. Gu, J. Shi, J. Mol. Catal. A: Chem. 322 (2010) 50–54.
[20] D.-H. Zhan, G.-D. Li, J.-X. Li, J.-S. Chen, Chem. Commun. 29 (2008) 3414–3416.
[21] C. Xu, J. Xie, D. Ho, C. Wang, N. Kohler, E.G. Walsh, J.R. Morgan, Y.E. Chin, S. Sun, Angew. Chem. Int. Ed. 47 (2008) 173–176.
[22] M. Wang, D. Guo, H. Li, J. Solid State Chem. 178 (2005) 1996–2000.
[23] H. Li, Z. Zhu, P. Li, X. Zhou, J. Colloid Interface Sci. 349 (2010) 613–619.
[24] M.-W. Xu, G.-Y. Gao, W.-J. Zhou, K.-F. Zhang, H.-L. Li, J. Power Sources 175 (2008) 217–220.
[25] C. Xu, Z. Tian, P. Shen, S.P. Jiang, Electrochim. Acta 53 (2008) 2610–2618.
[26] A.H. Lu, E.L. Salabas, F. Schuth, Angew. Chem. Int. Ed. 46 (2007) 1222–1245.
[27] J. Liu, B. Sun, J. Hu, Y. Pei, H. Li, M. Qiao, J. Catal. 274 (2010) 287–295.
[28] Y. Jang, J. Chung, S. Kim, S.W. Jun, B.H. Kim, D.W. Lee, B.M. Kim, T. Hyeon, Phys. Chem. Chem. Phys. 13 (2011) 2512–2516.
[29] B. Brandt, W. Ludwig, J.H. Fischer, J. Libuda, F. Zaera, S. Schauermann, J. Catal. 265 (2009) 191–198.
[30] J. Li, J. Ren, G. Yang, P. Wang, H. Li, X. Sun, L. Chen, J.T. Ma, R. Li, Mater. Sci. Eng. B 172 (2010) 207–212.
[31] N. Pinna, S. Grancharov, P. Beato, P. Bonville, M. Antonietti, M. Niederberger, Chem. Mater. 17 (2005) 3044–3049.
[32] W. Kalss, R. Haubner, G. Lippold, B. Lux, Diam. Relat. Mater. 7 (1998) 158–164.
[33] D. Bersani, P. Lottici, A. Montenero, J. Raman Spectrosc. 30 (1999) 355–360.
[34] J.A. Robinson, C.P. Puls, N.E. Staley, J.P. Stitt, M.A. Fanton, K.V. Emtsev, T. Seyller, Y. Liu, Nano Lett. 9 (2009) 964–968.
[35] I. Pastoriza-Santos, L.M. Liz-Marza, Nano Lett. 2 (2002) 903–905.
[36] Y. Gao, P. Jiang, L. Song, J. Wang, L. Liu, D. Liu, Y. Xiang, Z. Zhang, X. Zhao, X. Dou, J. Cryst. Growth 289 (2006) 376–380.
[37] M. Giersig, I. Pastoriza-Santos, L.M. Liz-Marzan, J. Mater. Chem. 14 (2004) 607–610.
[38] T. Masaharu, T. Xinling, M. Mika, M. Yoshinori, W. Midori, Cryst. Growth Des. 10 (2010) 5238–5243.
[39] I. Pastoriza-Santos, L.M. Liz-Marza, Langmuir 18 (2002) 2888–2894.
[40] J. Wu, F. Qin, G. Cheng, H. Li, J. Zhang, Y. Xie, H.J. Yang, Z. Lu, X. Yu, R. Chen, J. Alloys Compd. 509 (2011) 2116–2126.
[41] R. Hao, R. Xing, Z. Xu, Y. Hou, S. Gao, S. Sun, Adv. Mater. 22 (2010) 2729–2742.
[42] W. Niu, L. Zhang, G. Xu, ACS Nano 4 (2010) 1987–1996.
[43] D. Fritsch, K. Kuhr, K. Mackenzie, F.-D. Kopinke, Catal. Today 82 (2003) 105–118.
[44] H. Hildebrand, K. Mackenzie, F.-D. Kopinke, Appl. Catal. B: Environ. 91 (2009) 389–396.
[45] C. Wang, H. Daimon, S. Sun, Nano Lett. 9 (2009) 1493–1496.
[46] L. Piccolo, C.R. Henry, J. Mol. Catal. A: Chem. 167 (2001) 181–190.
[47] Y. Li, E. Boone, M.A. El-Sayed, Langmuir 18 (2002) 4921–4925.